

GaAsBi STRUCTURES FOR ULTRAFAST OPTOELECTRONICS GROWN AT DIFFERENT Bi FLUXES

S. Driukas ^a, V. Pačebutas ^a, S. Stanionytė ^b, B. Čechavičius ^a, A. Bičiūnas ^a, and G. Valušis ^c

^a Department of Optoelectronics, Center for Physical Sciences and Technology, Saulėtekio 3, 10257 Vilnius, Lithuania

^b Department of Characterization of Materials Structure, Center for Physical Sciences and Technology,
Saulėtekio 3, 10257 Vilnius, Lithuania

^c Institute of Photonics and Nanotechnology, Faculty of Physics, Vilnius University, Saulėtekio 3, 10257 Vilnius, Lithuania
Email: simonas.driukas@ftmc.lt

Received 10 December 2025; accepted 12 December 2025

GaAsBi is an attractive semiconductor material for the development of infrared optoelectronics devices due to possibilities of band engineering when, varying the Bi content, one can induce a rapid rising of the valence band edge. Although this property makes GaAsBi a promising material for terahertz (THz) emitters, telecommunication lasers, and low noise photodetectors, the yield of the developed GaAsBi-based devices is still low indicating a requirement for the better quality of the material. In this work, we extend previous studies focusing on the investigation of the influence of Bi flux during the molecular beam epitaxy growth. The structures were characterized using high-resolution X-ray diffraction, photoluminescence and optical pump–THz probe technique. It is shown that multiple growth runs targeting at the ~6% Bi content and near-infrared operation wavelength of around 1.2 μm yielded consistent structural and optical properties, indicating that the optimal and repeatable growth protocol has been successfully established. The observed red-shifts in photoluminescence spectra and the bi-exponential decay in carrier relaxation can be associated with the existence of band-tail states and random potential due to fluctuations in the distribution of Bi content.

Keywords: GaAsBi, high-resolution X-ray diffraction, photoluminescence, optical pump–THz probe

1. Introduction

GaAsBi (gallium arsenide bismide) is an attractive semiconductor material [1, 2] for the development of infrared optoelectronics devices due to possibilities of band engineering: by varying the Bi content within just a few percent [3], one can induce a rapid rising of the valence band edge through a band anticrossing interaction, which has a strong effect on the bandgap and the spin–orbit splitting [4]. This property makes GaAsBi a promising material for terahertz (THz) emitters, telecommunication lasers [5–7], low noise photodetectors [8], optoelectronic terahertz (THz) spectroscopic systems [9] among other devices [10]. As the reduction of the band gap occurs mainly from the valence band side, it has no strongly pronounced effect on the electron mobility, which remains in a range of 2000 cm^2/Vs [11]. It indicates that GaAsBi compounds can be an engaging semiconductor

choice for ultrafast optoelectronic devices [12]. THz photoconducting switches, the wavelength of which lies in the range of 1 to 1.5 μm , developed as compact laser sources – both solid-state and fibre ones – are available for this range [13]. This would allow one to reduce the size of spectroscopic THz systems if compared to conventional Ti-sapphire laser-based setups making thus THz spectroscopic technique compact and more convenient in practical use. However, the development of GaAsBi-based devices has run into quality issues of the material with sufficiently large Bi fractions when low substrate temperatures are required for the structure growth [14, 15].

Therefore, there has been a large variety of efforts dedicated for the progress in development of quality GaAsBi structures. It was shown that annealing of bismides at 600°C and higher temperature leads to the reduction of trapping times shorter than 1 ps [16]. Since electron trapping times in

GaAsBi can be varied via thermal annealing of the layers, THz time-domain spectroscopy systems using Yb:KGW and Yb-doped fibre lasers to excite GaAsBi structures with 6% Bi at 1030 nm wavelength were demonstrated [17, 18]. As the yield of the fabricated devices was found low, it encouraged systematic technological studies mainly focused on the influence of technological parameters on the crystalline structure, morphology, surface roughness, optical properties, and peculiarities of carrier dynamics of thick GaAsBi layers [19]. As far as our knowledge goes, there was no dedicated study on Bi flux related effects on the optical/electronic properties of GaAsBi structures.

In this work, we centre our attention on the influence of Bi flux during the molecular beam epitaxy growth of GaAsBi compounds and the possible effect on their optical/electronic properties. Here, series of different samples were designed, grown and investigated: 6 samples were thin films with a target thickness of 100 nm while two other ones were GaAs/GaAsBi quantum wells (QWs) with a target well thickness of 15 nm. Structures were characterized using high-resolution X-ray diffraction, photoluminescence and optical pump–THz probe technique. It is revealed that multiple growth runs targeting the ~6% Bi content and the near-infrared operation wavelength of around 1.2 μm yielded consistent structural and optical properties, indicating that a stable and repeatable growth protocol has been successfully established. The observed red-shifts in photoluminescence spectra and the bi-exponential decay in carrier relaxation can be associated with the existence of band-tail states and random potential is due to fluctuation in the distribution of Bi content in the materials.

2. Methods and experimental techniques

2.1. Growth of GaAsBi films

All samples were grown using a solid source Veeco GENxplor molecular beam epitaxy (MBE) system equipped with an As valved cracker and conventional dual filament bismuth and gallium sources. The samples were grown on a quarter of 2" semi-insulating (001) GaAs substrates. The substrate temperature was monitored using a thermocouple and with a kSA BandIt broadband pyrometry module. The experimental procedure involved outgassing

each substrate before the growth at temperatures ranging from 600 to 620°C (only BandIt temperature readings are referred to from this point onwards) under As_2 flux in order to eliminate native oxides. A layer of GaAs buffer material with a thickness of approximately 100 nm was deposited on GaAs substrates at 580°C temperature. The adjustment of the Ga/As ratio was performed on a calibration substrate through the observation of RHEED pattern transition by varying the position of the As valve aiming to achieve unity, which is required for the growth of GaAsBi layers. The bismuth concentration was varied by adjusting the bismuth flux in a range of 6.8×10^{-8} Torr to 8.7×10^{-8} Torr. The exact Bi flux values for each sample are displayed in Table 1. The growth rate has been set at approximately 500 nm/h for all bismide layers. The substrate temperature was maintained within a range of 300–320°C during the bismide growth phase. The same growth procedure was used for the growth of the quantum well (QW), except that, once the QW had been grown, the temperature of the substrate was increased to 440°C and a 80 nm-thick GaAs cap layer was grown. Overall, 8 samples were grown and characterized, 6 samples were thin films with a target thickness of 100 nm, while two other samples were GaAs/GaAsBi quantum wells (QWs) with a target well thickness of 15 nm.

2.2. Characterization of the samples by optical techniques

Photoluminescence (PL) was measured employing a standard experimental setup. A diode-pumped solid-state laser with a wavelength of 532 nm, and a maximum intensity of 5 kW cm^{-2} was used as the excitation source [20]. Experiments were performed at room temperature.

To study carrier relaxation dynamics in the grown GaAsBi layers, optical pump–THz probe (OPTP) experiments were performed. A 70 fs duration, 76 MHz repetition rate and 1030 nm central wavelength Yb:KGW (ytterbium-doped potassium gadolinium tungstate) *Light Conversion* PHAROS oscillator served as a pump source keeping the excitation power at 450 mW. An optical pump was further passed through a 1.9 mm diaphragm. The same laser was used for the excitation of the THz emitter and detector branches with mechanical delay lines for the precise optical path control. A *TERAVIL*-produced THz

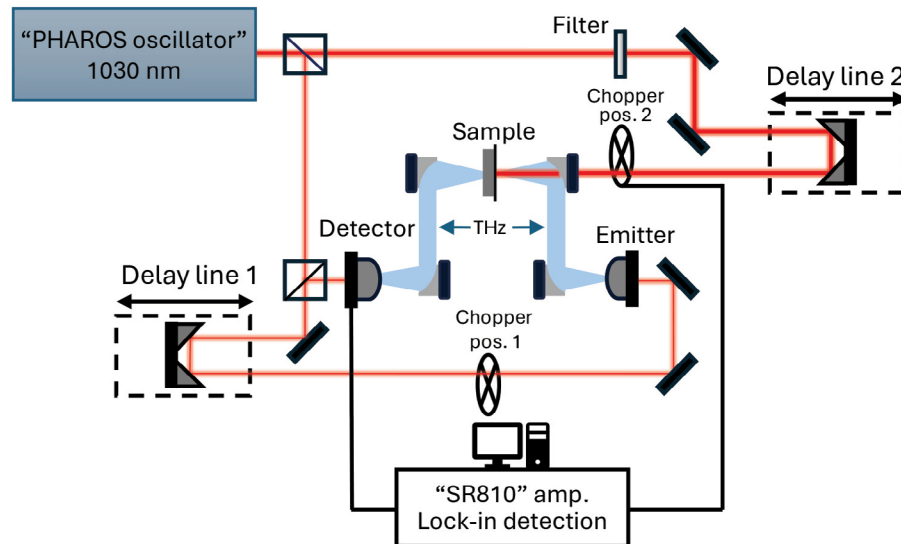


Fig. 1. Experimental setup of the optical pump–THz probe measurement. Chopper position was changed through the experiment. For setup calibration, the chopper was kept in the emitter branch (position 1) to set the required delay after which it was moved to position 2 to measure the pump–probe kinetics.

detector and emitter were used as well as a Stanford instruments 810 lock-in amplifier for noise reduction. The experimental setup is depicted in Fig. 1.

3. Experimental results and discussion

3.1. Material characterization

To determine the quality and structure of the grown GaAsBi samples high-resolution X-ray diffraction (HR XRD) ω - 2θ scans were analyzed. The concentration of Bi and the thickness of the GaAsBi layer were assessed by fitting the experimental result. The measured XRD spectra reveal distinct peaks arising from the GaAs substrate as well as GaAsBi layers. A clear shift of the GaAsBi peak is observed with increasing the Bi concentration, indicating an

increased lattice expansion arising from a rather large ionic radius of the Bi atoms. The thickness of the GaAsBi layers was 95–102 nm as determined by XRD interference oscillations. For QW samples, the thickness of GaAsBi well was 12 and 14 nm for 4.5 and 6.8% Bi concentration, respectively. The samples with a lower Bi concentration than 6% displayed a slightly poorer crystal quality – the XRD peaks are wider, and in the case of VGA1505 no interference oscillations are visible. A similar picture, without clearly resolved oscillations, is seen also for the 8.5% Bi content sample. It seems that at 6–7% Bi concentration the GaAsBi lattice becomes more robust and resistant to major dislocations and defects, producing sharper XRD peaks compared to lower or higher concentration samples.

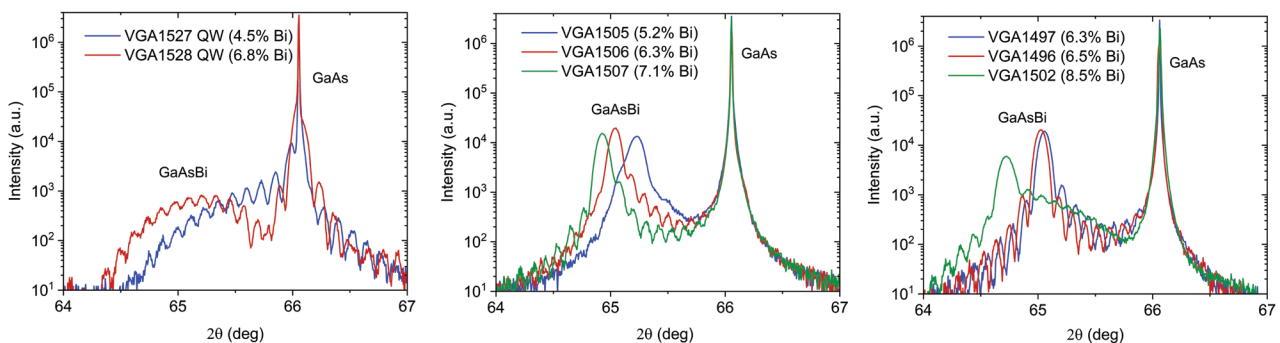


Fig. 2. ω - 2θ diffraction scans of (004) plane. GaAs substrate and GaAsBi peaks are named accordingly. The exact Bi content of the sample was evaluated by fitting the XRD results as displayed in the graph legends.

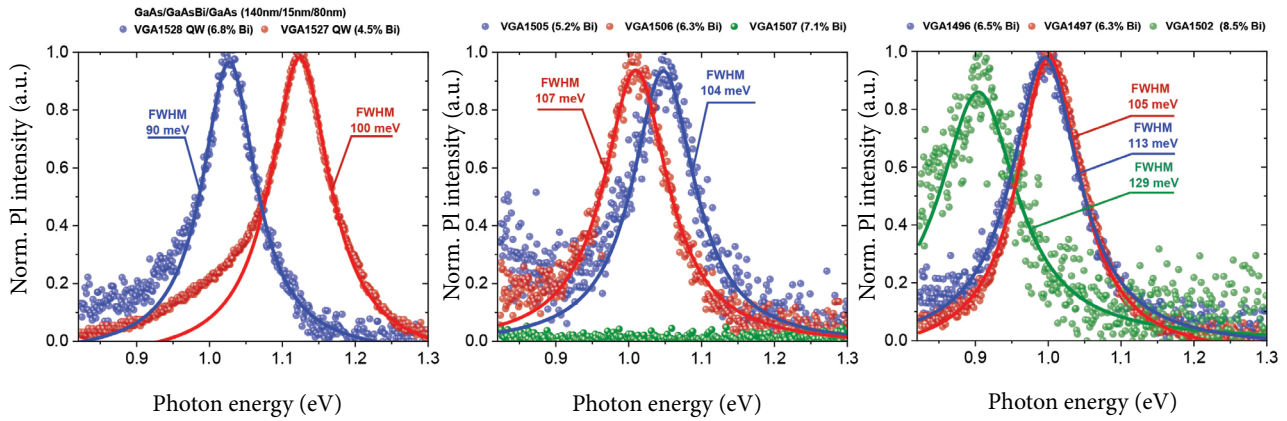


Fig. 3. Photoluminescence spectra of grown GaAsBi samples. Scatter plots denote the experimental results while theoretical fitting curves are displayed as continuous lines. Full-width half-maximum (FWHM) values for each sample are indicated graphically. All the peaks were modelled as Lorentzian shapes to account for the broadening of the emission due to disorder and defects [24]. Note the arising mismatch of the fit and experimental data at the lower energy tail of the PL peaks while the higher energy side is in good agreement. Such asymmetry is likely to be induced by the band-tail effects of the GaAsBi layers, therefore the appearing PL extension into lower energies cannot be fitted by a symmetrical Lorentzian function and requires an additional in-depth theoretical analysis.

3.2. Photoluminescence study

The PL spectra are depicted in Fig. 3. It is seen that the results are fairly similar for all the grown GaAsBi thin films with PL emission in the near-infrared region (NIR) from 1.1 to 1.37 μm . Full-width half-maximum (FWHM) values slightly varied around 107 meV with the exception of VGA1502 sample, which had a substantially higher Bi concentration of 8.5% and a peak PL emission at 1348 nm. In this case, the PL peak is wider, with FWHM of 129 meV, indicating a lower crystal quality in accordance with the XRD result. One can note that for the higher concentration sample of 7.1% Bi and high Bi flux values, no PL emission is detected. It can be associated with the increase of non-radiative recombination centres due to the growth at lower substrate temperatures.

Taking into account the empirical law describing the GaAsBi bandgap [21, 22],

$$E_g^{(\text{GaAs}_{1-x}\text{Bi}_x)}(x) = 1.625 - 2.3x - \sqrt{0.04 + 2.56x}, \quad (1)$$

Bi fraction values are evaluated assuming E_g values as the peak PL energies. It is observed that the values extracted from the PL peak positions differ from those obtained through the XRD model fitting. The corresponding Bi fractions and the discrepancies between the two measurement methods are summarized in Table 1.

As illustrated in the Table, the quantity of bismuth incorporated is influenced by two factors: the bismuth flow and the growth temperature. It has been observed that, at constant growth temperature, an increase in the bismuth flux results in a greater quantity of bismuth being incorporated. An increase in the growth temperature, maintained at a constant bismuth flow rate, results in a slight reduction in the amount of bismuth incorporated. This phenomenon can be attributed to the loss of bismuth from the wetting layer into the environment during the growth process.

All the grown films exhibit PL peaks that are red-shifted relative to the XRD-derived estimates as XRD results were analyzed taking into account the compressive strain of the layers. Careful look reveals not only the red-shift of the PL lines but also they display a slightly asymmetrical shape – emission is stretched into the lower energy regions. A similar behaviour was observed in the GaAsBi structures in lower Bi content (3.3 and 4.8%), and it was attributed to the band-tail states [22]. As seen, there are some differences between the estimates of Bi concentration via XRD and PL techniques due to the difference in approaches. Note that for the Bi concentrations above 7% the PL ‘sees’ higher Bi concentration than the XRD. Moreover, the PL spectral lines are rather broad indicating a random distribution of Bi atoms in

Table 1. Varied MBE growth parameters of GaAsBi samples, the peak PL emission as well as the calculated Bi % fraction from the PL spectra and XRD fitting. The difference is defined as the PL data calculation minus the XRD fit result. The abbreviation QW in the sample title indicates that it contains a quantum well.

Sample	Bi flux during growth, Torr 10^{-8}	Growth temperature, °C	Bi fraction from XRD fit, %	Bi fraction from PL data, %	Difference, %	Peak PL emission wavelength, nm	Peak PL emission energy, eV
VGA1496	7.2	314.5	6.5	6.98	-0.48	1244	0.997
VGA1497	7.2	317.5	6.3	6.92	-0.62	1240	1
VGA1502	7.9	314	8.5	8.81	-0.31	1367	0.907
VGA1505	7.2	321	5.2	5.94	-0.74	1181	1.05
VGA1506	7.8	320	6.3	6.72	-0.42	1228	1.01
VGA1507	8.7	305	7.1	-	-	-	-
VGA1527QW	6.8	316.5	4.5	4.58	-0.08	1104	1.123
VGA1528QW	7.8	306.5	6.8	6.43	0.37	1210	1.025

the structures. Therefore, the occurrence of localized states via the random potential [25] and the presence of band-tail states from the intrinsic band-edge are suspected to drive optical and electrical properties which are of essential importance for the performance of GaAsBi-based devices.

A different behaviour is observed in the PL emission from the GaAsBi QWs. In this case, both samples exhibit smaller FWHM values, and a reduced discrepancy between the Bi fractions obtained from PL and XRD measurements. It can be caused by substantially thinner layers which are potentially more resistant to major defects which effectively strain the lattice still not reaching the breaking limit due to a very limited layer thickness. Additionally, the QW confinement modifies the electronic structure, and the appearance of discrete energy levels may account for the blue-shifted PL emission relative to the bulk-like thin-film samples.

Overall, multiple growth runs targeting the ~6% Bi content and the near-infrared operation wavelength of around $1.2 \mu\text{m}$ yielded consistent structural and optical properties, indicating that a stable and repeatable growth protocol has been successfully established.

3.3. Optical pump-THz probe technique

To get a deeper insight into possible effects on carrier transport properties, carrier decay peculiarities were studied using the optical pump-THz probe technique. The THz absorption decay curves

are presented in Fig. 4. For the VGA1528 and VGA1527 QW samples, the signal was too low to effectively measure carrier decay, thus the results are not displayed. For the rest of the samples, a bi-exponential decay can be assumed, described as

$$I(t) = A_1 e^{-\frac{t}{\tau_1}} + A_2 e^{-\frac{t}{\tau_2}}, \quad (2)$$

where $\tau_{1,2}$ denote the decay component time constants and $A_{1,2}$ are the component amplitudes.

The fitting results are displayed in Table 2.

As seen, the transient absorption decay starts with a fast initial component with the characteristic time of tens of ps followed by a much slower decay extending into the nanosecond scale. For the samples with Bi concentration of ~6%, results are fairly similar. The same transient shape can be observed, and the characteristic decay parameters differ only slightly. However, the VGA1506 sample showed a stronger THz probe absorption indicating a higher concentration of excited carriers and, therefore, a better compound quality. An opposite effect can be seen for the samples with a higher Bi concentration. In these samples, the signal amplitude is lower, and the shape of the decay is different. The amplitude of the initial fast decay A_1 is smaller, and the longer component dominates, leading to a longer decay time compared to that of other samples. At higher Bi concentrations, the fluctuations in Bi content distribution began to play a role revealing itself as long tails in carrier decay dynamics.

More specifically, this becomes more pronounced when the Bi concentration reaches more

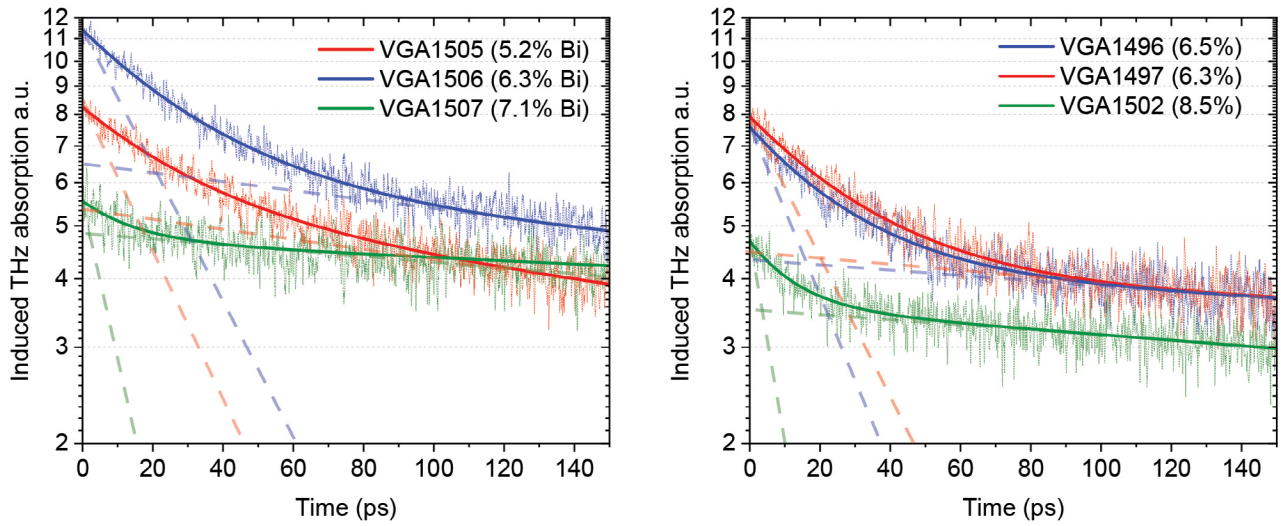


Fig. 4. Induced THz absorption measured by optical pump–THz probe technique. Experimental data is represented by short-dashed lines while a wide continuous line denotes the bi-exponential decay fit. Fast and slow decay components are schematically represented by dashed straight lines as a guide to the eye.

than ~7%. A reason of the effect can be related to the random potential [25, 26] and also the possible formation of Bi-dimers with the increase of Bi content [27]. As a result, after carrier excitation, they rapidly recombine, and at certain level, carriers are not able to screen the random potential. Therefore, it causes their spatial separation, thus preventing the carrier recombination rate and making the diffusion rather slow. The estimates indicated (Table 2) that relaxation times can extend into the ns time scale. This is illustrated via two relaxation slopes indicated via dashed straight lines presented in Fig. 4 plots.

Usually, samples with a lower crystal quality display shorter carrier lifetimes due to a higher concentration of defects and carrier trap centres. This behaviour is evident in samples VGA1502 (8.5% Bi) and VGA1507 (7.1% Bi). As summarized in Table 2, the time constants of the initial

decay component in these samples are approximately half compared to the rest of the group. When considered together with their reduced THz absorption by excited free carriers, these observations indicate a higher defect concentration related to the higher Bi flux.

Therefore, not only the band-tail states from the intrinsic band-edge can drive optical and electrical properties of GaAsBi structures – the influence of Bi content random distribution, and, in particular, at higher concentrations, exceeding 7%, can be important and affect the performance and operation speed of GaAsBi-based devices. Despite of the fact that carrier localization effect is getting considerable attention [20, 28–30], the role of random potential in carrier transport properties and possible effects on devices operation still needs a systematic investigation and a separate debate.

Table 2. The results of Bi-exponential fit of carrier decay measured by an optical pump–THz probe.

Sample	τ_1 , ps	A_1	τ_2 , ns	A_2	$T_{\text{substr.}}$, °C
VGA1496	28.7	3.48	0.89	2.74	314.5
VGA1497	34.5	4.02	0.88	1.57	317.5
VGA1502	13.2	1.15	0.95	3.87	314
VGA1505	33.7	3	0.47	4.97	321
VGA1506	35.8	5.58	0.56	4.34	320
VGA1507	15.1	0.85	0.81	2.81	305

4. Conclusions

Molecular beam epitaxy grown GaAsBi heterostructures were systematically characterized to establish the optimal growth protocol suitable for high-frequency optoelectronic applications. The bismuth content from 4.5 to 8.5% was intentionally varied to assess the influence of Bi incorporation on structural and optical properties in the near infrared of 1.1–1.4 μm .

HRXRD measurements revealed that the Bi compositions in a range of 6–7% yield the highest crystal quality. This conclusion is supported by photoluminescence measurements, where samples with a similar Bi content exhibited narrower PL linewidths compared to those with a higher Bi content. Time-resolved carrier-decay measurements indicated two components – the fast one, on the ps timescale, related to the increase of recombination centres, while the second, with longer times within 0.5–0.95 ns, in the samples with higher Bi concentrations, likely can be related to the formation of the random potential at the Bi content above ~7%. The results demonstrate that the GaAsBi layers with 6–7% Bi content provide the most favourable combination of structural quality and fast carrier dynamics, making this composition range optimal for ultrafast optoelectronic device applications. The possible role of the random potential in carrier transport properties and the potential influence on device operation needs a systematic investigation and a separate debate.

References

- [1] K. Oe and H. Okamoto, New semiconductor alloy $\text{GaAs}_{1-x}\text{Bi}_x$ grown by metal organic vapor phase epitaxy, *Jpn. J. Appl. Phys.* **37**, L1283–L1285 (1998).
- [2] S. Tixier, M. Adamczyk, T. Tiedje, S. Francoeur, A. Mascarenhas, Peng Wie, and F. Schiettekatte, Molecular beam epitaxy growth of $\text{GaAs}_{1-x}\text{Bi}_x$, *Appl. Phys. Lett.* **82**, 2245–2247 (2003).
- [3] S. Francoeur, M.-J. Seong, A. Mascarenhas, S. Tixier, M. Adamczyk, and T. Tiedje, Band gap of $\text{GaAs}_{1-x}\text{Bi}_x$, $0 < x < 3.6\%$, *Appl. Phys. Lett.* **82**, 3874–3876 (2003).
- [4] Y. Liu, X. Yi, N.J. Bailey, Z. Zhou, T.B.O. Rockett, L.W.Lim, Ch.H. Tan, R.D. Richards, and J.P.R. David, Valence band engineering of GaAsBi for low noise avalanche photodiodes, *Nat. Commun.* **12**, 4784 (2021), <https://doi.org/10.1038/s41467-021-24966-0>
- [5] P. Ludewig, N. Knaub, N. Hossain, S. Reinhard, L. Nattermann, I.P. Marko, S.R. Jin, K. Hild, S. Chatterjee, W. Stolz, S.J. Sweeney, and K. Volz, Electrical injection $\text{Ga}(\text{AsBi})/(\text{AlGa})\text{As}$ single quantum well laser, *Appl. Phys. Lett.* **102**, 242115 (2013).
- [6] T. Fuyuki, R. Yoshioka, K. Yoshida, and M. Yoshimoto, Long-wavelength emission in photo-pumped $\text{GaAs}_{1-x}\text{Bi}_x$ laser with low temperature dependence of lasing wavelength, *Appl. Phys. Lett.* **103**, 202105 (2013).
- [7] R. Butkutė, A. Geižutis, V. Pačebutas, B. Čechavičius, V. Bukauskas, R. Kundrotas, P. Ludewig, K. Volz, and A. Krotkus, Multi-quantum well $\text{Ga}(\text{AsBi})/\text{GaAs}$ laser diodes with more than 6% of bismuth, *Electron. Lett.* **50**, 1155–1157 (2014).
- [8] A. Geižutis, V. Pačebutas, R. Butkutė, P. Svidovskys, V. Strazdienė, and A. Krotkus, Growth and characterization of UTC photo-diodes containing $\text{GaAs}_{1-x}\text{Bi}_x$ absorber layer, *Solid St. Electron.* **99**, 101–103 (2014).
- [9] A. Urbanowicz, V. Pačebutas, A. Geižutis, S. Stanionytė, and A. Krotkus, Terahertz time-domain-spectroscopy system based on 1.55 μm fiber laser and photoconductive antennas from dilute bismides, *AIP Adv.* **6**, 0250218 (2016), <https://doi.org/10.1063/1.4942819>
- [10] R.D. Richards, N.J. Bailey, Y. Liu, T.B.O. Rockett, and A.R. Mohmad, GaAsBi: From molecular beam epitaxy growth to devices, *Phys. Status Solidi B* **259**, 2100330 (2022), <https://doi.org/10.1002/pssb.202100330>
- [11] D.G. Cooke, F.A. Hegmann, E.C. Young, and T. Tiedje, Electron mobility in dilute GaAs bismide and nitride alloys measured by time-resolved terahertz spectroscopy, *Appl. Phys. Lett.* **89**(12), 122103 (2006), <https://doi.org/10.1063/1.2349314>
- [12] K. Bertulis, A. Krotkus, G. Aleksejenko, V. Pačebutas, R. Adomavičius, G. Molis, and S. Marcinkevičius, GaBiAs: A material for optoelectronic terahertz devices, *Appl. Phys. Lett.* **88**(20), 201112 (2006), <https://doi.org/10.1063/1.2205180>

- [13] A. Krotkus, Semiconductors for terahertz photonics applications, *J. Phys. D* **43**(27), 273001 (2010), <https://doi.org/10.1088/0022-3727/43/27/273001>
- [14] R. Butkutė, V. Pačebutas, B. Čechavičius, R. Adomavičius, A. Koroliov, and A. Krotkus, Thermal annealing effect on the properties of GaBiAs, *Phys. Status Solidi C* **9**, 1614 (2012), <https://doi.org/10.1002/pssc.201100700>
- [15] E. Dudutienė, A. Jasinskas, B. Čechavičius, R. Nedzinskas, M. Jokubauskaitė, A. Bičiūnas, V. Bukauskas, G. Valušis, and R. Butkutė, Photoluminescence properties of GaAsBi single quantum wells with 10% of Bi, *Lith. J. Phys.* **61**, 142–150 (2021), <https://doi.org/10.3952/PHYSICS.V61I2.4442>
- [16] B. Čechavičius, R. Adomavičius, A. Koroliov, and A. Krotkus, Thermal annealing effect on photoexcited carrier dynamics in $\text{GaBi}_x\text{As}_{1-x}$, *Semicond. Sci. Technol.* **26**(8), 085033 (2011), <https://doi.org/10.1088/0268-1242/26/8/085033>
- [17] V. Pačebutas, A. Bičiūnas, S. Balakauskas, A. Krotkus, G. Andriukaitis, D. Lorenc, A. Pugžlys, and A. Baltuška, Terahertz time-domain-spectroscopy system based on femtosecond Yb: fiber laser and GaBiAs photoconducting components, *Appl. Phys. Lett.* **97**(3), 031111 (2010), <https://doi.org/10.1063/1.3458826>
- [18] V. Pačebutas, A. Bičiūnas, K. Bertulis, and A. Krotkus, Optoelectronic terahertz radiation system based on femtosecond 1 μm laser pulses and GaBiAs detector, *Electron. Lett.* **44**(19), 1154 (2008), <https://doi.org/10.1049/el:20081630>
- [19] S. Stanionytė, A. Vailionis, V. Bukauskas, S. Tumėnas, A. Bičiūnas, A. Arlauskas, R. Butkutė, and A. Krotkus, Thick epitaxial GaAsBi layers for terahertz components: The role of growth conditions, *Lith. J. Phys.* **58**(1), 126–134 (2018), <https://doi.org/10.3952/physics.v58i1.3658>
- [20] E. Dudutienė, A. Jasinskas, S. Stanionytė, M. Skapas, A. Vaitkevičius, B. Čechavičius, and R. Butkutė, Impact of elevated GaAs barrier growth temperature on the homogeneity and photoluminescence of GaAsBi multiple quantum wells, *Mat. Sci. Semicond. Proc.* **199**, 109828 (2025).
- [21] A.R. Mohmad, F. Bastiman, C.J. Hunter, R.D. Richards, S.J. Sweeney, J.S. Ng, J.P.R. David, and B.Y. Majlis, Localization effects and band gap of GaAsBi alloys, *Phys. Status Solidi B* **251**(6), 1276–1281 (2014), <https://doi.org/10.1002/pssb.201350311>
- [22] A. Mohmad and J.P.R. David, Bandgap engineering of GaAsBi alloy for emission of up to 1.52 μm , in: *Proceedings of IEEE International Conference on Semiconductor Electronics* (IEEE, 2018).
- [23] B. Yan, X. Chen, L. Zhu, L. Wang, M. Wang, S. Wang, and J. Shao, Unraveling band-tail effects on temperature-dependent emission in GaAsBi via photoluminescence, *Adv. Sci.* e16349 (2025), <https://doi.org/10.1002/ADVS.202516349>
- [24] J. Michael Hollas, *Modern Spectroscopy* (Wiley, New Jersey, 2004).
- [25] B.I. Shklovskii and A.L. Efros, *Electronic Properties of Doped Semiconductors* (Springer-Verlag, Berlin, 1984).
- [26] J.A. Nixon and J.H. Davies, Potential fluctuations in heterostructure devices, *Phys. Rev. B* **41**, 7929–7933 (1990), <https://doi.org/10.1103/PhysRevB.41.7929>
- [27] F. Bastimann, A.G. Cullis, J.P.R. David, and S.J. Sweeney, Bi incorporation in GaAs(100)- 2×1 and 4×3 reconstructions investigated by RHEED and STM, *J. Cryst. Growth* **341**, 19–23 (2012), <https://doi.org/10.1016/j.jcrysgro.2011.12.058>
- [28] M. Karaliūnas, E. Dudutienė, A. Čerškus, J. Pagalys, S. Pūkienė, A. Udal, R. Butkutė, and G. Valušis, High precision parabolic quantum wells grown using pulsed analog alloy grading technique: Photoluminescence probing and fractional-dimensional space approach, *J. Lumin.* **239**, 118321 (2021), <https://doi.org/10.1016/j.jlumin.2021.118321>
- [29] M. Jokubauskaitė, G. Petrusėvičius, A. Špokas, B. Čechavičius, E. Dudutienė, and R. Butkutė, Effects of parabolic barrier design for multiple GaAsBi/AlGaAs quantum well structures, *Lith. J. Phys.* **63**, 264–272 (2023), <https://doi.org/10.3952/physics.2023.63.4.8>
- [30] M. Jansson, S. Hiura, J. Takayama, A. Murayama, F. Ishikawa, W.M. Chen, and I.A. Buyanova, Dynamics of strongly localized excitons in GaAs/GaAsBi core/shell nanowires, *J. Phys. Chem. C* **129**, 4456–4463 (2025).

GaAsBi DARINIAI ITIN SPARČIAI OPTOELEKTRONIKAI, IŠAUGINTI ESANT SKIRTINGIEMS Bi SRAUTAMS

S. Driukas^a, V. Pačebutas^a, S. Stanionytė^b, B. Čechavičius^a, A. Bičiūnas^a, G. Valušis^c

^a *Fizinių ir technologijos mokslų centro Optoelektronikos skyrius, Vilnius, Lietuva*

^b *Fizinių ir technologijos mokslų centro Medžiagų struktūrinės analizės skyrius, Vilnius, Lietuva*

^c *Vilniaus universiteto Fizikos fakulteto Fotonikos ir nanotechnologijų institutas, Vilnius, Lietuva*

Santrauka

GaAsBi yra patraukli puslaidininkinė medžiaga infraraudonųjų spindulių optoelektronikos įtaisams kurti dėl juostų inžinerijos galimybių, o keičiant Bi kiekį galima efektyviai susiaurinti draustinės juostos tarpą. Nors ši savybė daro GaAsBi perspektyvia medžiaga terahercų (THz) spinduliuotės šaltiniams, telekomunikacijų lazeriams ir mažo triukšmo fotodetektoriams, iki šiol sukurtų GaAsBi pagrindu pagamintų įtaisų našumas išlieka nedidelis, o tai rodo geresnės medžiagos kokybės poreikį. Šiame darbe tęsiami ankstesni tyrimai, daugiau dėmesio skiriant Bi srauto įtakai molekulių pluoštų epitaksijos augimo metu. Dariniai buvo charakterizuoti naudojant rentgeno spindulių difrakcijos, fotoluminescencijos ir optinio žadinimo–THz zondavimo metodus. Bismuto koncentracija bandiniuose buvo keičiama nuo

4,5 iki 8,5 %, siekiant nustatyti optimalias sluoksnių auginimo sąlygas ir įvertinti Bi įterpimo įtaką medžiagos kokybei.

Optinio žadinimo–THz zondavimo matavimai parodė, kad egzistuoja du krūvininkų relaksacijos sandai: greitas (dešimtys ps) ir lėtas (0,5–0,95 ns). Manoma, kad greitas sandas susijęs su padidėjusiu rekombinacijos centrų skaičiumi, o lėtas – su galimu fliuktuacinio potencialo formavimusi.

Parodyta, kad daugkartiniai auginimai, orientuoti į ~6 % Bi kiekį darinyje ir maždaug 1,2 μm artimojo infraraudonojo spinduliavimo veikimo bangos ilgį, leidžia užauginti darinius, turinčius stabilią struktūrą ir norimas optines savybes bei trumpus, ps trukmės, gyvavimo laikus.